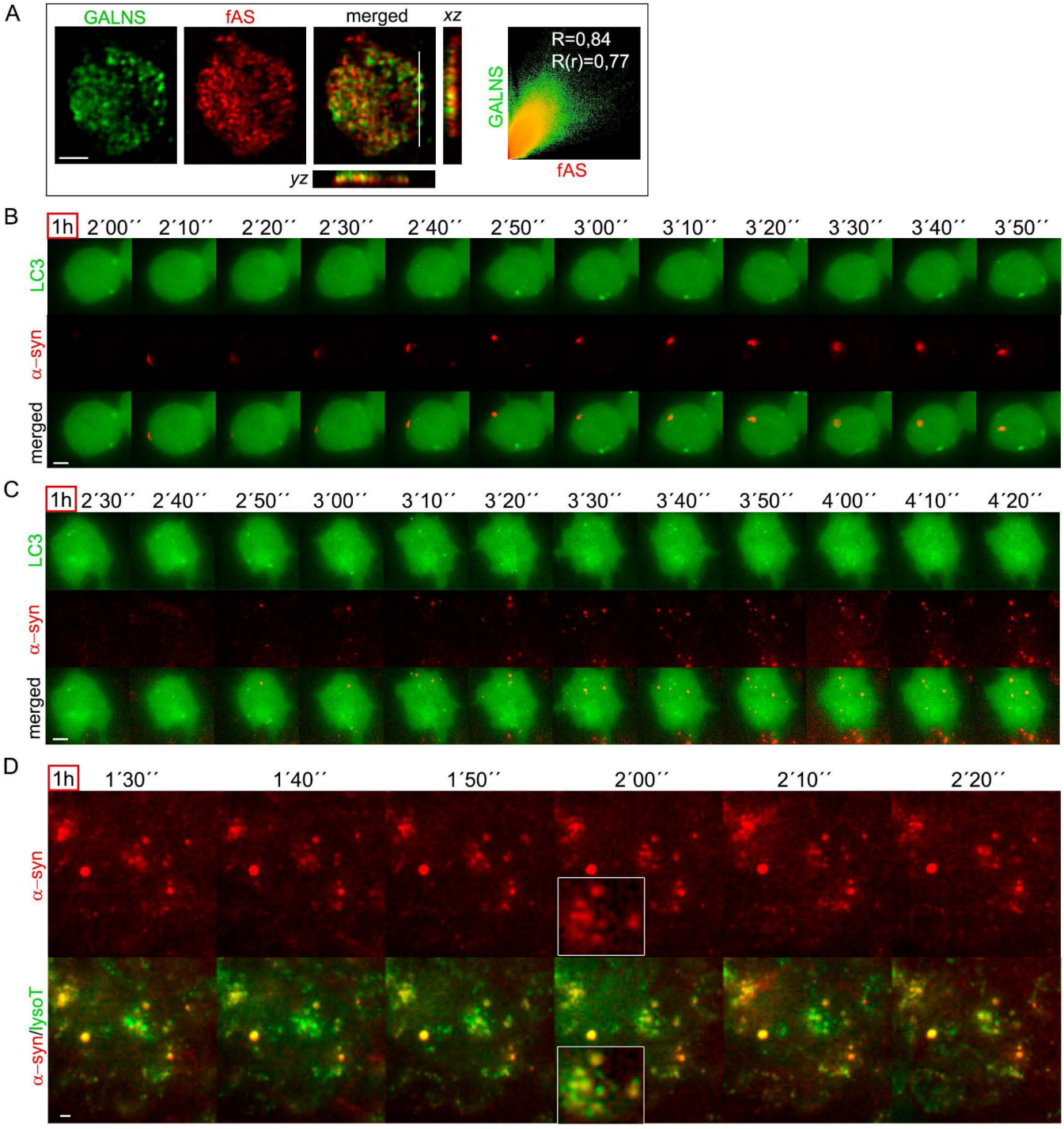

Figure S1.

Additional evaluation of lysosomal markers and autophagy dynamics of fAS-stimulated BV2 GFP-LC3 cells during early time points.

(A) Primary microglial cells were stimulated with fAS for 12h and co-localization between lysosomal specific marker GALNS and fAS was analysed by confocal microscopy. Pearson coefficient (R) and Overlap coefficient (R[r]) are listed. Scale bar, 5μm.

(B, C, D). BV2 GFP-LC3 (green) cells were stimulated with fAS (1uM, red) for 1h. Imaging started immediately after cellular stimulation and it was performed at 1 frame per 10 s during 1h, a selected interval within this sequence is shown. (C) shows fAS (red) and LysoTracker staining (green) of BV2 GFP-LC3 cells stimulated and imaged as described above. Of note that synuclein/LysoTracker co-localization is quickly observable after cellular internalization.

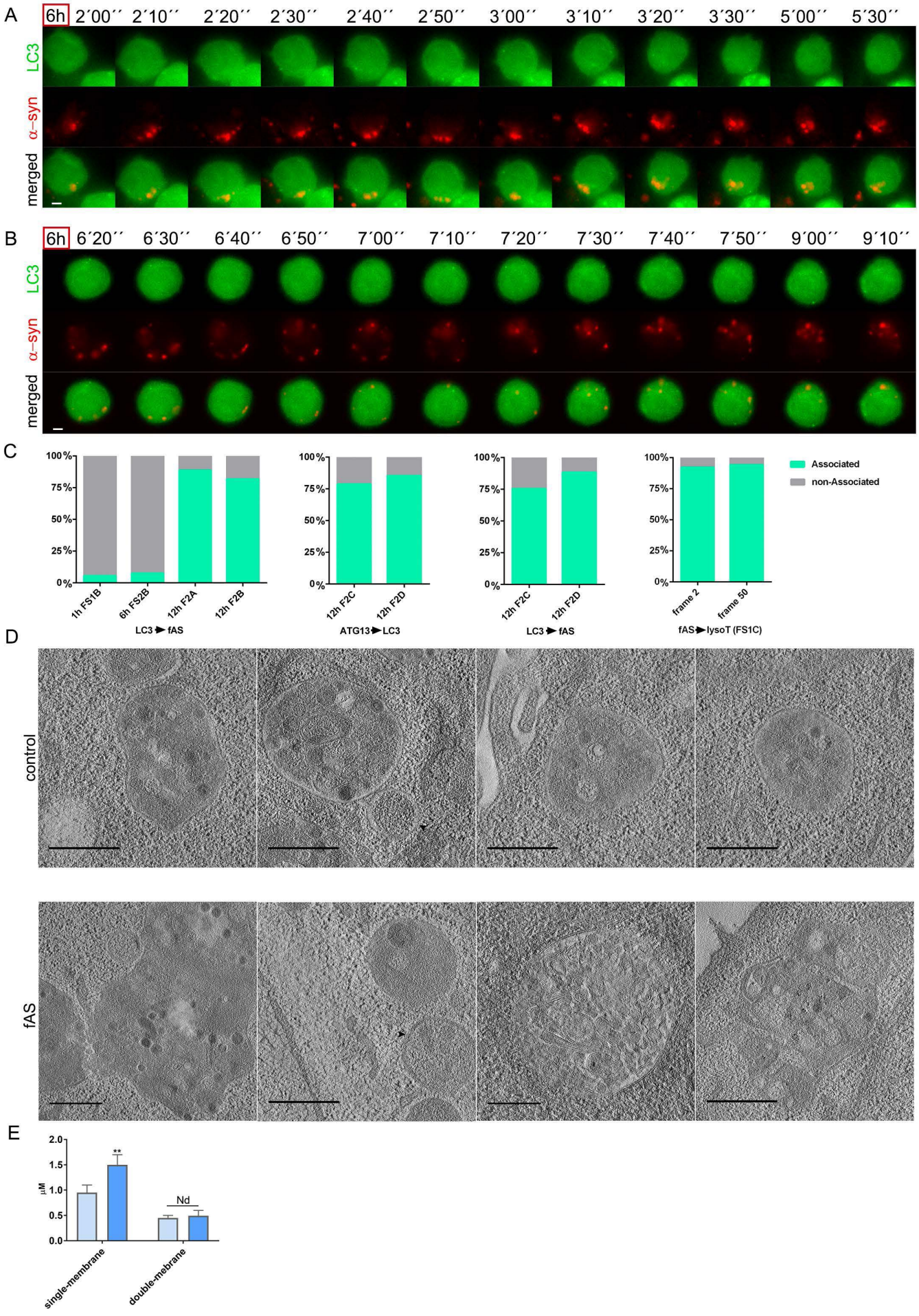

Figure S2.

Autophagy dynamics of fAS-stimulated BV2 GFP-LC3 cells during early time points (cont.) and comparison of single and double-membrane vesicles found in control and stimulated BV2 microglial cells.

A, B. BV2 GFP-LC3 (green) cells were stimulated with fAS (red) for 6h and imaged at 1 frame per 10 s during 1h, a selected interval within this sequence is shown. Scale bar, 2μm. (C) Values are percentages of association of LC3-positive vesicles with fAS; ATG13-positive vesicles with LC3; and fAS with LysoTracker-positive vesicles corresponding to analysis of time-lapse experiments from the indicated figures. (D) Representative images from EM tomograms of control and fAS-stimulated BV2 GFP-LC3 microglial cells showing different single and double membrane AV (scale bar, 500nm). (E) Graphs show the AV size quantification in both conditions. Results were analysed by one-way ANOVA followed by Post-Hoc Dunnet´s test; n = 30. Error bars represent SEM (*, $P < 0.05$; **, $P < 0.01$).

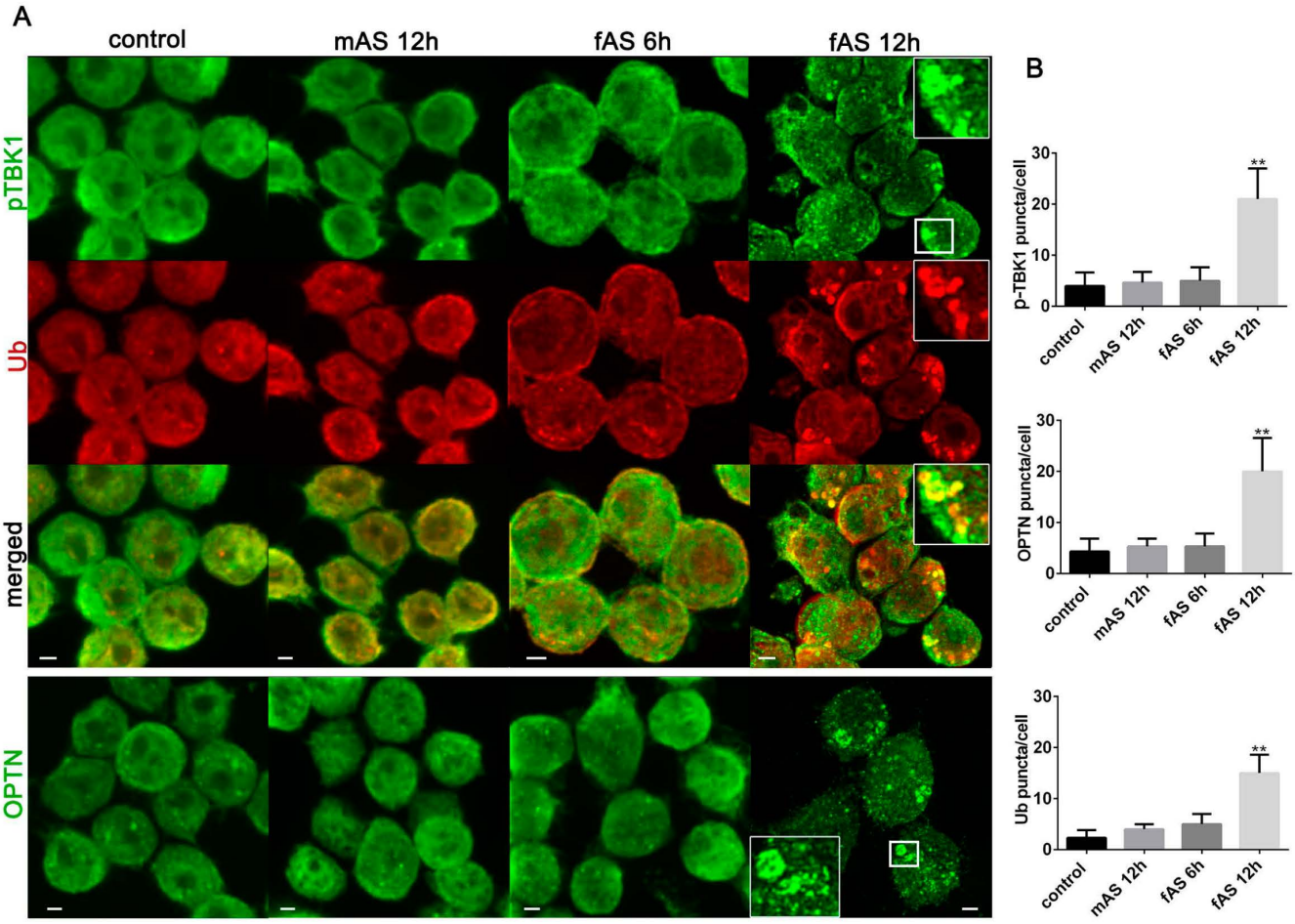

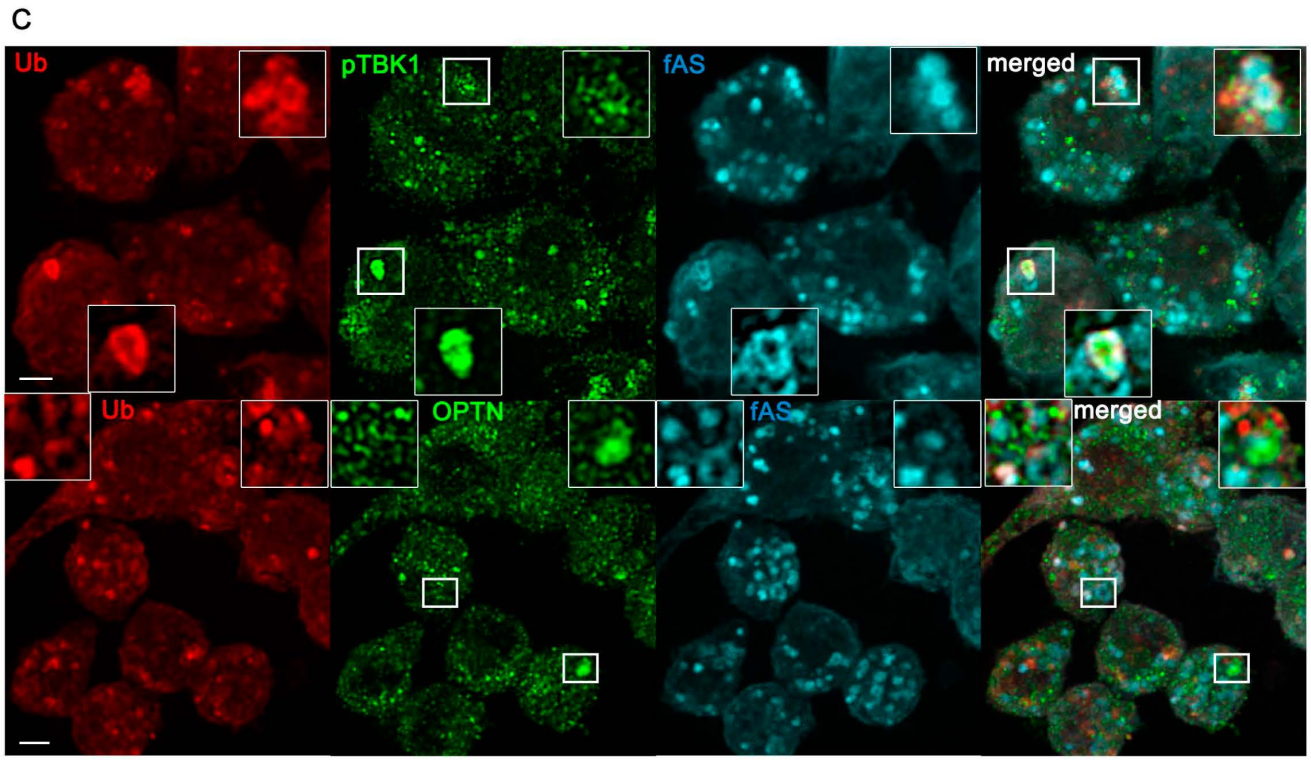

Figure S3.

OPTN and pTBK1 are recruited to lysosomal damage sites in fAS-stimulated microglial cells.

(A, B). BV2 cells were left untreated or stimulated with fibrillar (f) or monomeric (m) AS at the indicated time points. After that, cells were immunostained for pTBK1, ubiquitin (Ub) and OPTN. Puncta formation were determined using ImageJ particle counting plugin (B). Results were analysed by one-way ANOVA followed by Post-Hoc Dunnet´s test; n = 3. Error bars represent SEM (**, $P < 0.01$). (C) BV2 cells were stimulated with fAS (cyan) for 12h and were then fixed and stained for ubiquitin, pTBK1 and OPTN. Image crops shows magnification of the selected areas (white box).

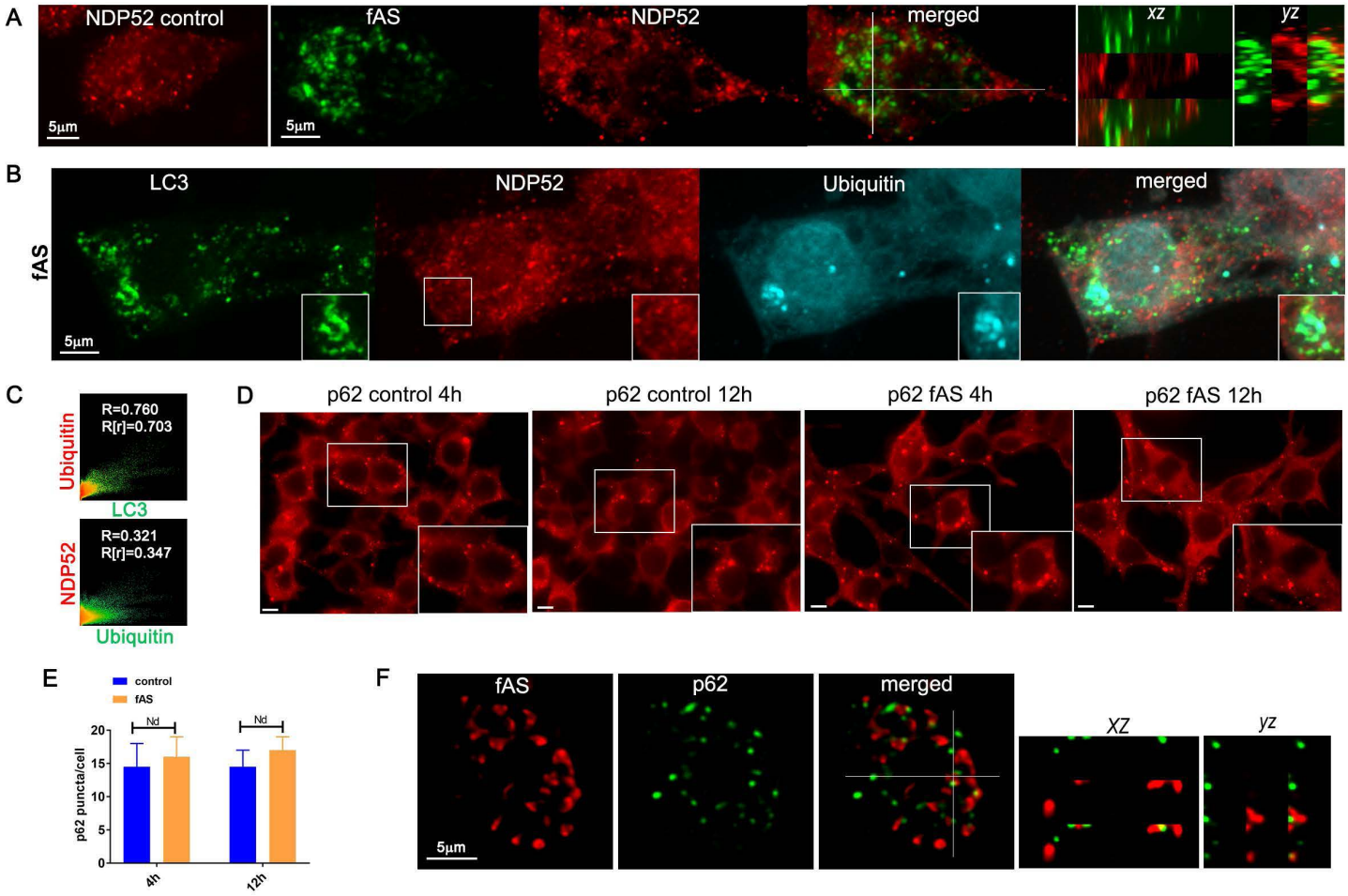

Figure S4.

NDP52 and p62 evaluation in fAS-stimulated microglial cells. (A) BV2 microglial cells were stimulated with fAS (green) for 12h. After that, cells were fixed and stained for NDP52 (red) and co-localization analysed with orthogonal views from z-stack confocal images. (B, C) fAS-stimulated BV2 GFP-LC3 cells were immunostained for NDP52 (red) and ubiquitin (cyan). (C) shows co-localization analysis of the selected area (white square) indicated in (B). Pearson coefficient (R) and Overlap coefficient (R[r]) are listed. (D, E) BV2 cells were stimulated with fAS (5µm) at the indicated time points or left untreated. Cells were then fixed and stained for p62 and p62-positive vesicles were quantified as shown in (E). (F) primary microglial cells were stimulated with fAS for 12h and stained for p62 (green). Co-localization was analysed with orthogonal views from z-stack confocal images after cellular deconvolution. A representative image sequence is shown (n=20).

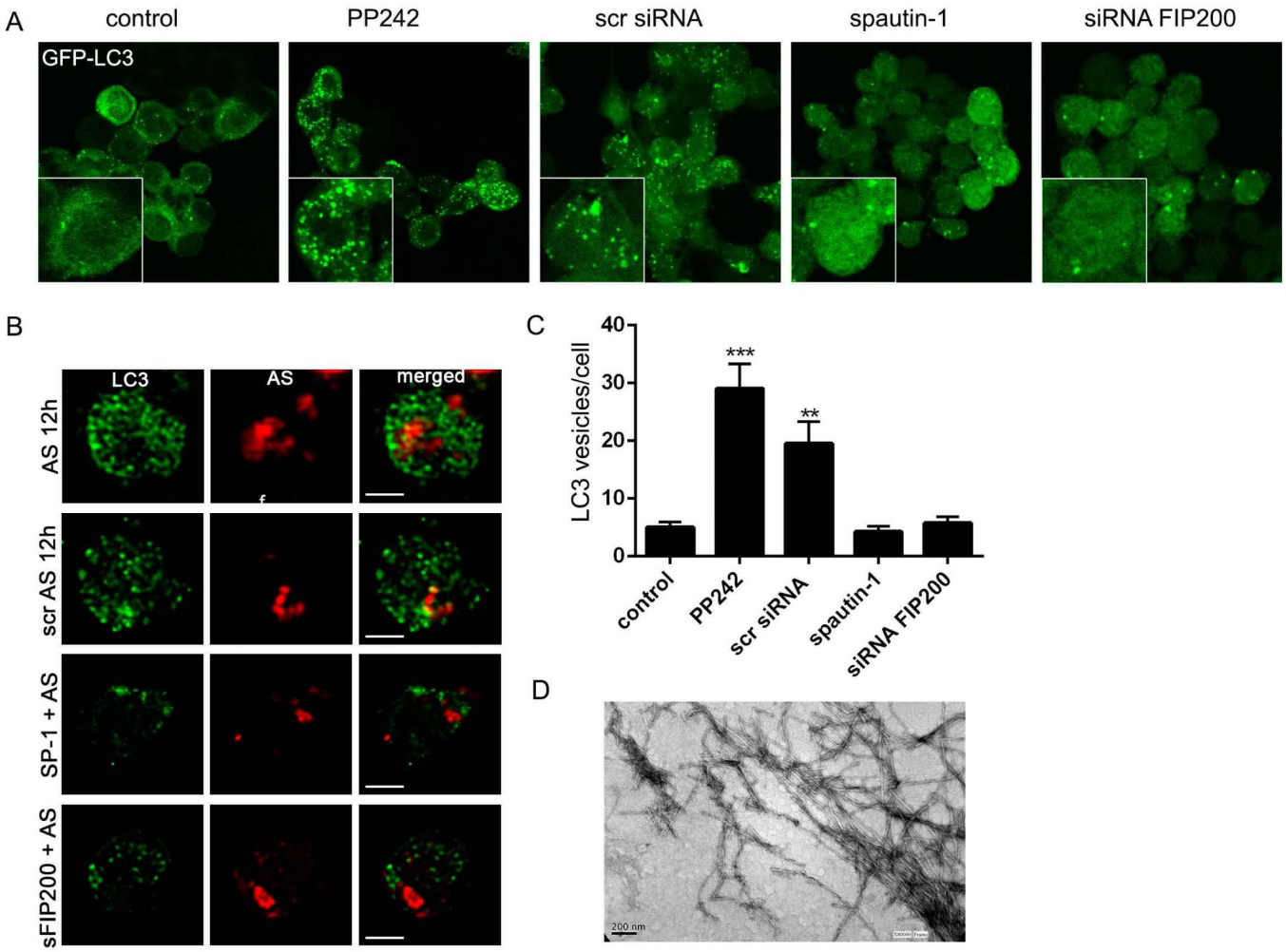

Figure S5.

Effects of spautin-1 and siRNAFIP200 on LC3 puncta induction.

(B) Representative Immunofluorescence images of BV2 GFP-LC3 cells treated with the mTOR inhibitor PP242 (1uM) for 3h in the presence or the absence of spautin-1 (10 μM) or siRNA FIP200. Spautin-1 and siRNA FIP200 were added 24h and 48 h before autophagy stimulation, respectively. (C) primary microglial cells were cultured in the presence or the absence of spautin-1 (10 μM) or siRNA FIP200 and stimulated with fAS (red, 5uM). After 12h, cells were immunostained for LC3 (green) and confocal images after cellular deconvolution are shown, scale bar, 5μm. (D) shows LC3 puncta quantification of the conditions indicated in (B). (E) TEM of fAS (scale bar, 200nm). Results were analysed by one-way ANOVA followed by Post-Hoc Dunnet´s test; n = 3. Error bars represent SEM (**, $P < 0.01$; ***, $P < 0.001$).

(Movies 1-9) Video files showing autophagy dynamics at different time points after fAS stimulation of BV2 microglial cells.

Movie 1

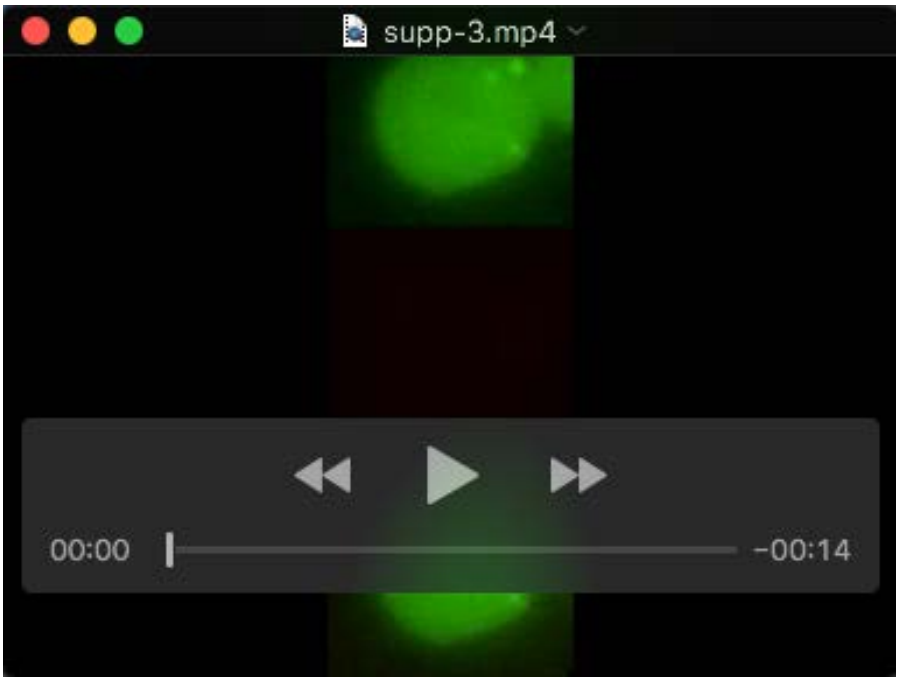

Movie 2

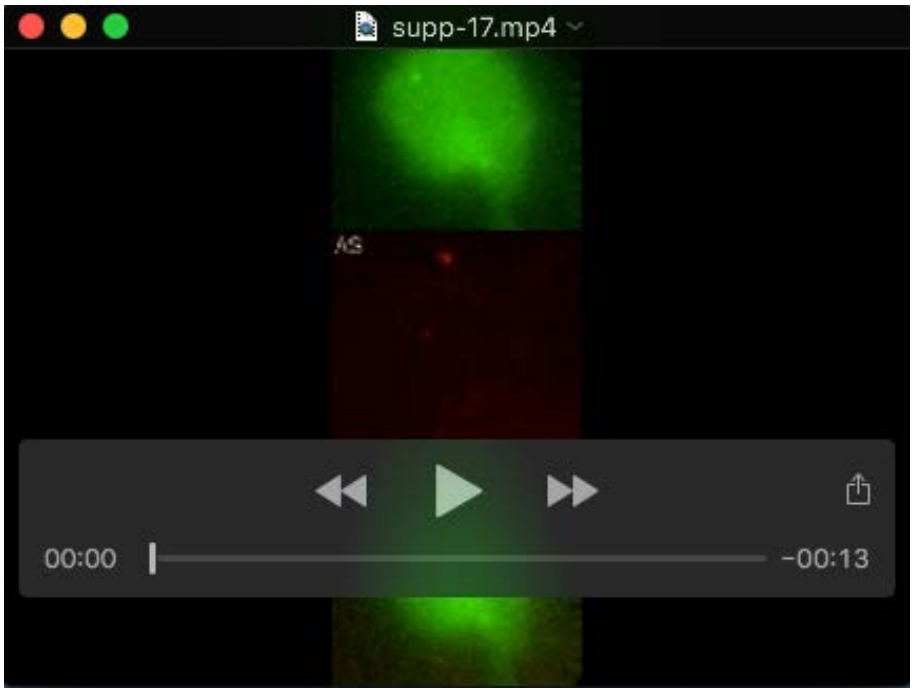

Journal of Cell Science • Supplementary information

Movie 3

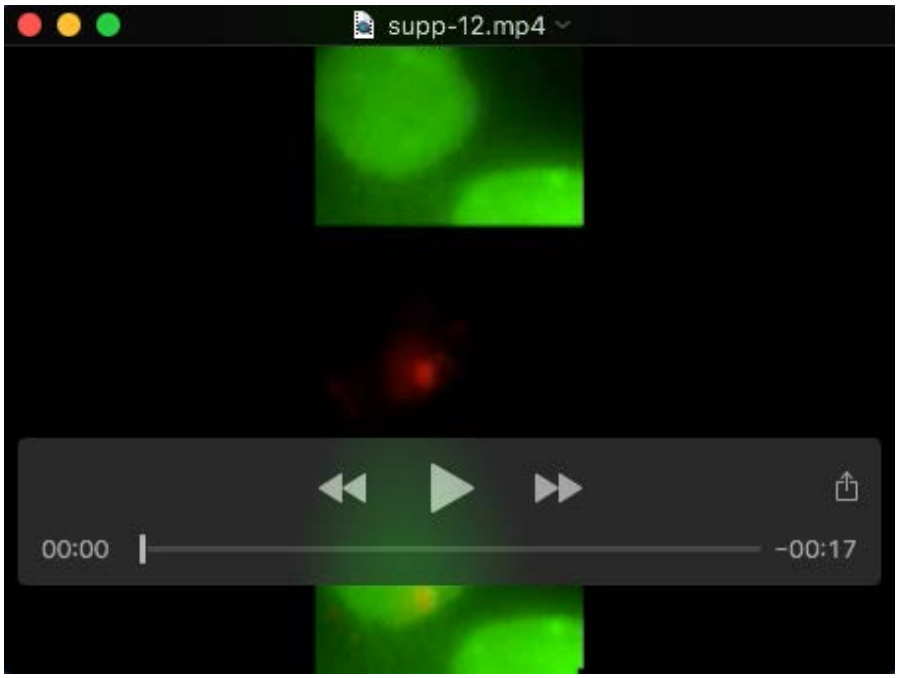

Movie 4

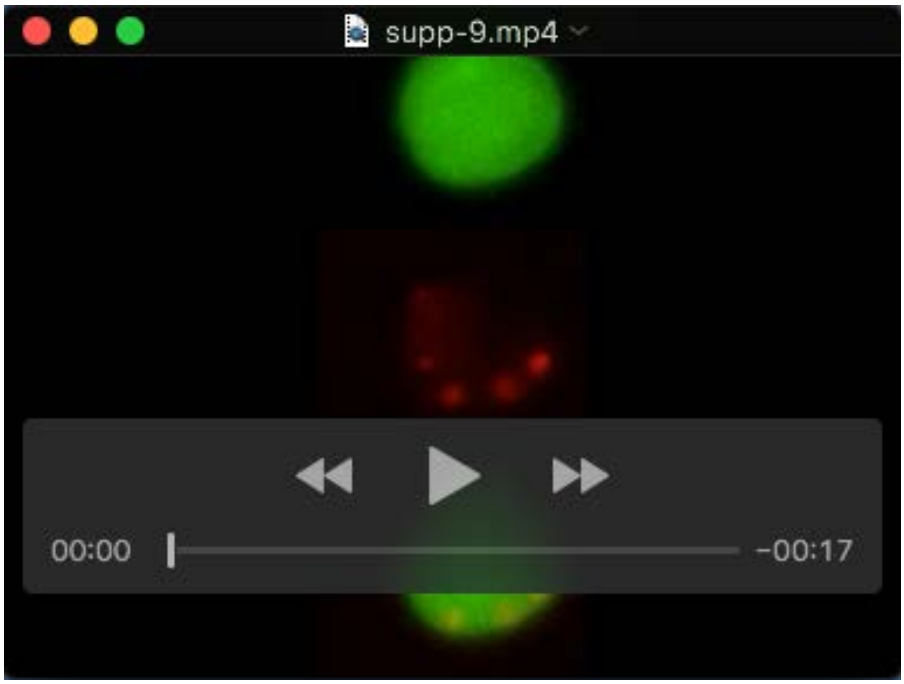

Movies 1, 2, 3 and 4. BV2 GFP-LC3 cells (green) were stimulated with fAS (red) and imaged immediately (Movie 1 and 2) or 6h after stimulation (Movie 3 and 4). Of note that no significant change in the dynamics of autophagy is detected over time, unlike long-term stimulation.

Movie 5

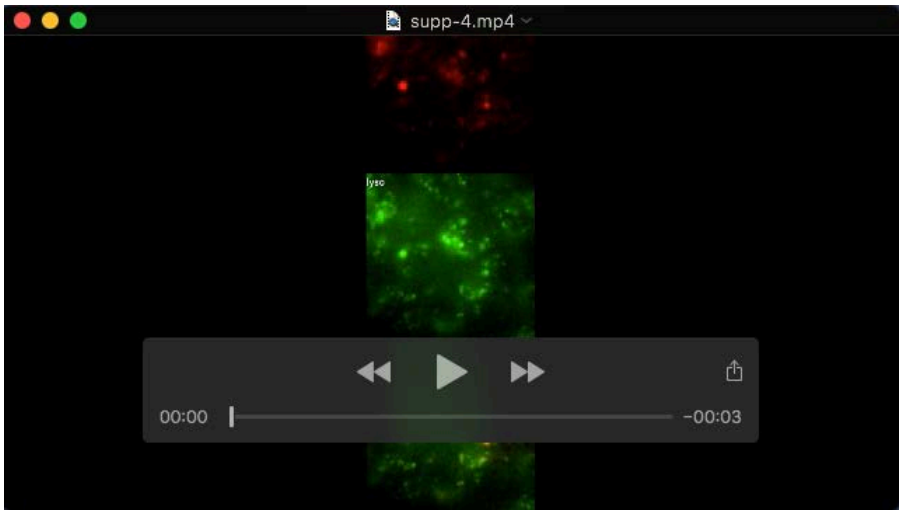

Movie 5. BV2 GFP-LC3 cells were stimulated with fAS (red) and imaged immediately after stimulation for 1h. LysoTracker (green) was used for lysosomal staining.

Movie 6

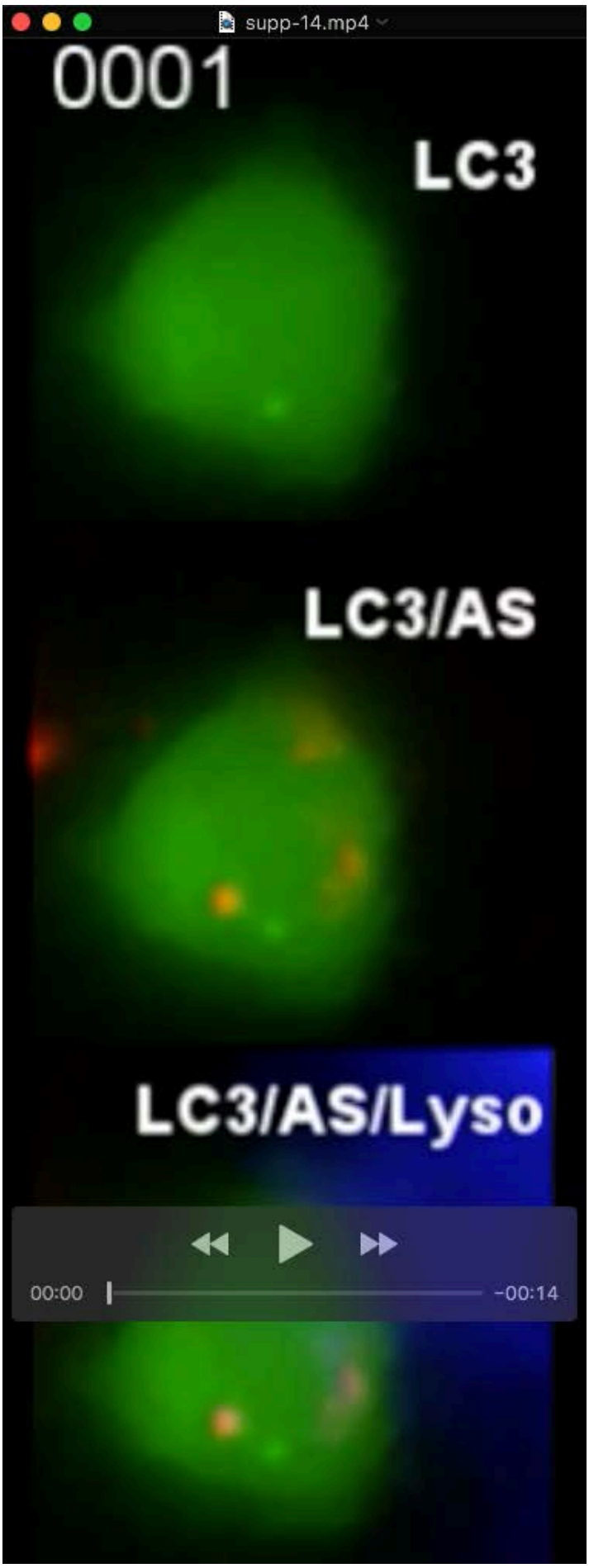

Journal of Cell Science • Supplementary information

Movie 7

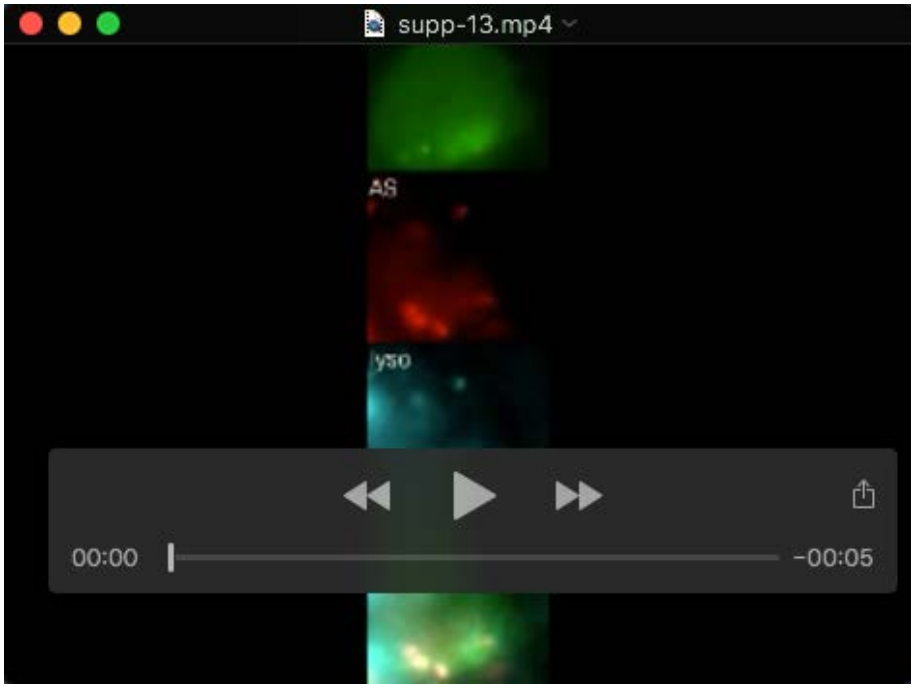

Movies 6 and 7. BV2 GFP-LC3 cells were stimulated with fAS for 12h and imaged at 1 frame per 10 s during 1h. Movie 6 and 7 correspond to the sequence shown in Fig. 2A and Fig. 2B, respectively. Of note that LC3 (green) forms a ring-like structure around fAS (red). LysoTracker (blue) was used for lysosomal staining.

Movie 8

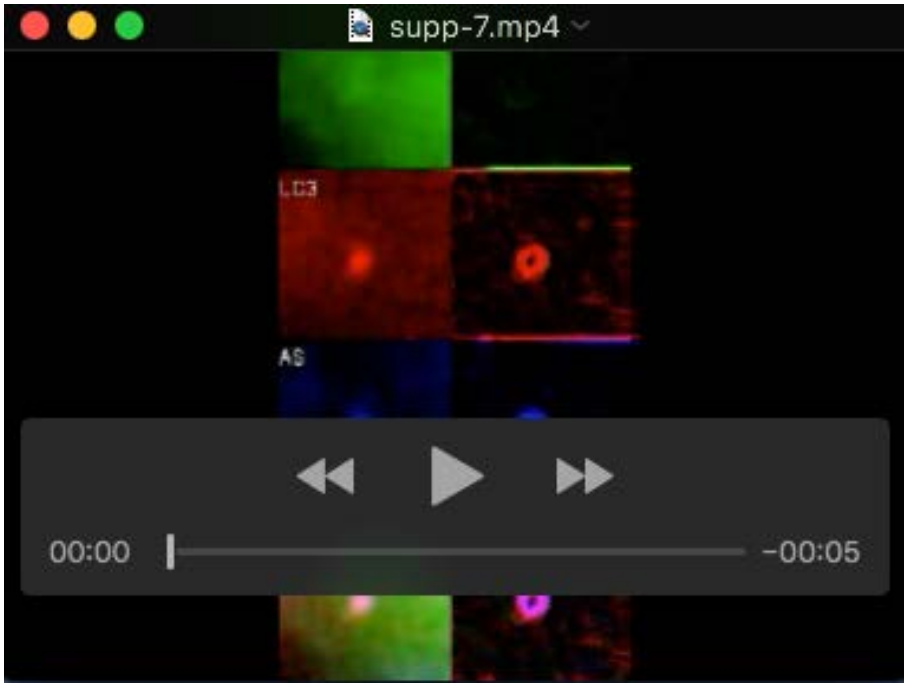

Movie 9

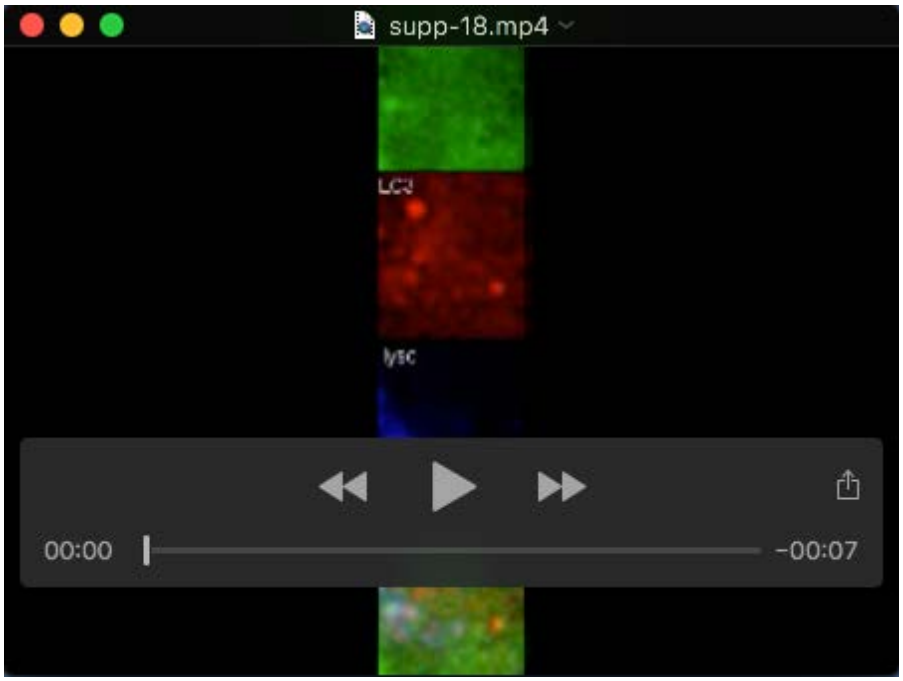

Movies 8 and 9. BV2 cells stably expressing ATG13 (green) were co-transfected with CFP-LC3 plasmid (red). Microglial cells were stimulated with fAS (blue) for 12h and imaged at 1 frame per 10 s during 1h. Movie 8 and 9 correspond to sequence shown in Fig. 2C and Fig. 2D, respectively. Of note that ATG13-positive structures mature into LC3-positive vesicles.

Movie 10

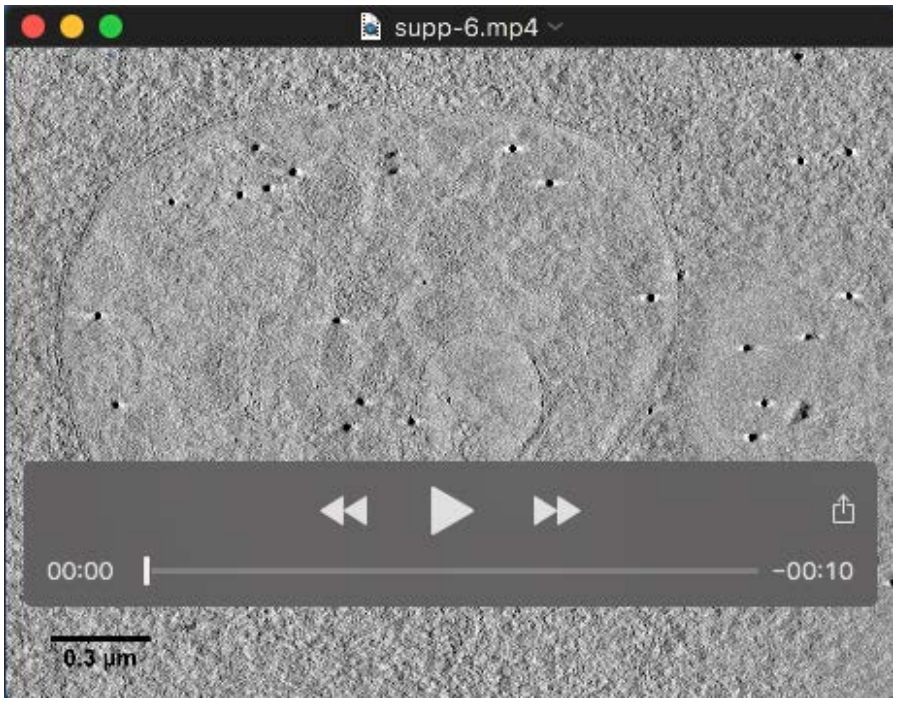

Movie 11

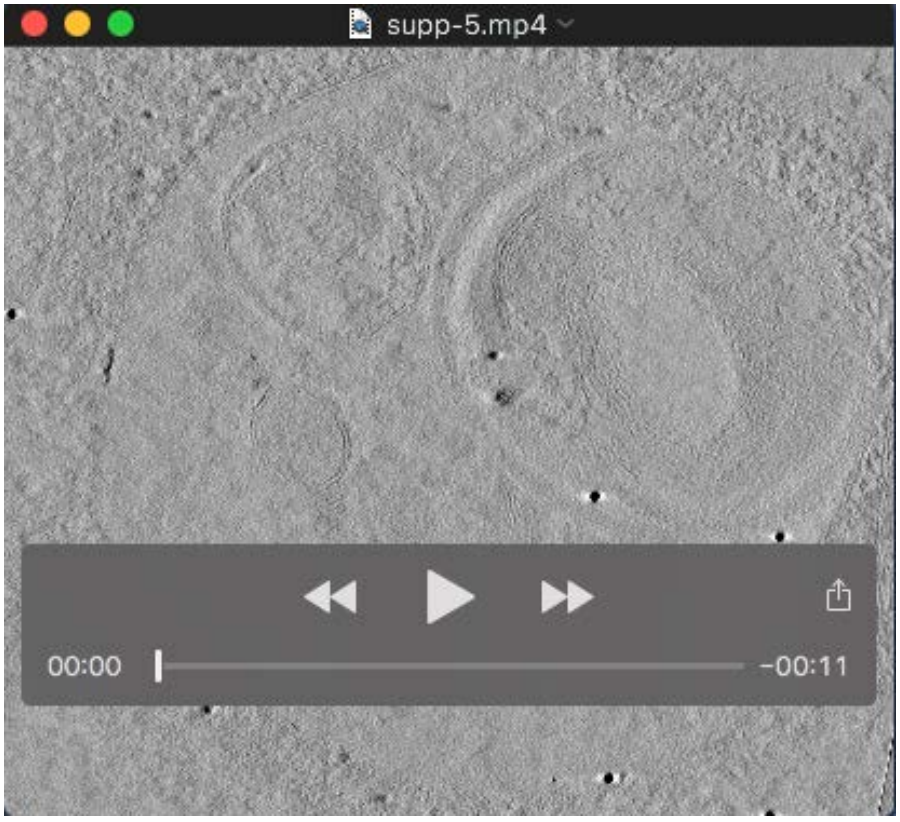

Journal of Cell Science • Supplementary information

Movie 12

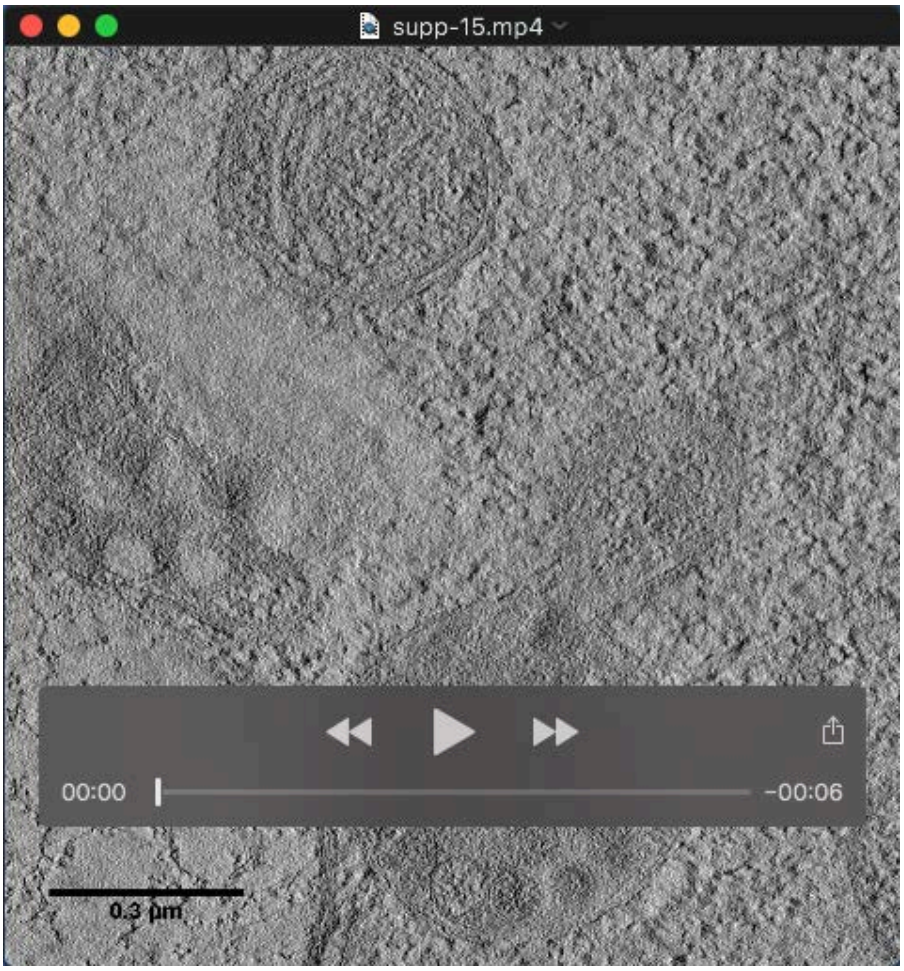

Movie 13

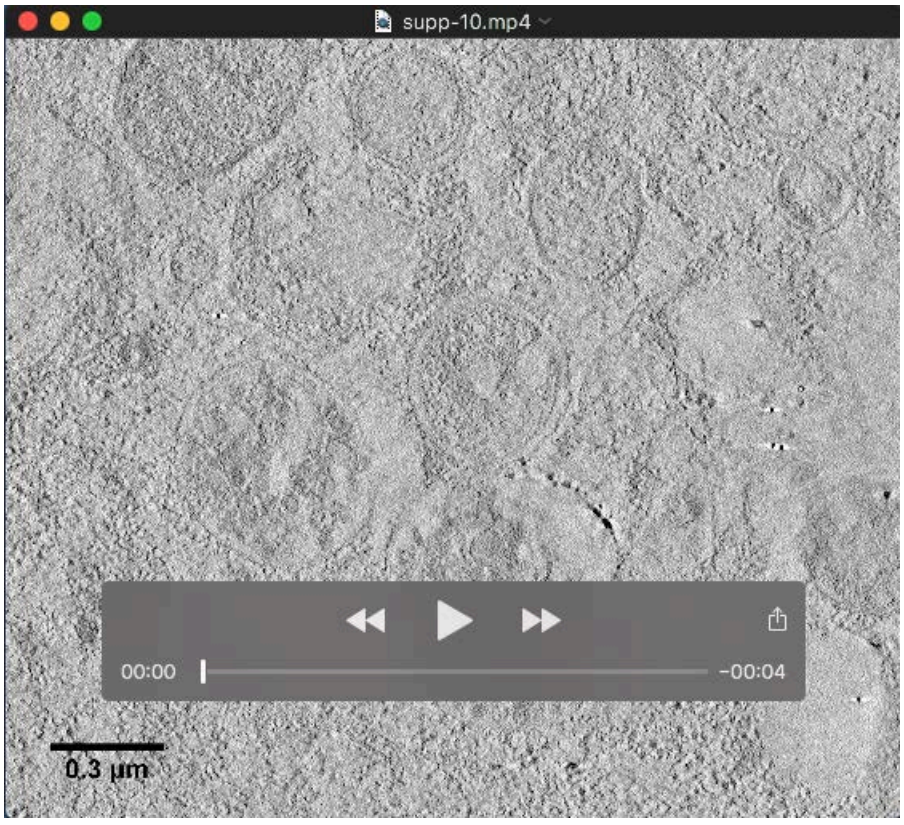

Journal of Cell Science • Supplementary information

Movies 10 – 13. EM tomograms from fAS-stimulated microglial cells.

EM high-magnification (20000X) tomograms corresponding to the images indicated as Fig. 3A (Movie 10), Fig. 3B (Movie 11), Fig. 3E (Movie 12) and Fig. 3G (Movie 13) are shown as video files. Of note, the presence of double membrane autophagosomes.

Movie 14

Movie 15

Movies 14, 15. Live imaging video file (Movie 14) and serial tomogram and 3D model (Movie 15) corresponding to Fig 4A and Fig. 4E, respectively. Tomograms of twenty consecutive 300nm sections were acquired at 9400X magnification and later aligned. Movie 15 shows a central double-membrane autophagosome containing several vesicles.

Movie 16

Movie 17

Movies 16 and 17. Live imaging video file (Movie 16) and serial tomogram and 3D model (Movie 17) corresponding to Fig. 4C and Fig. 4H, respectively. Movie 17 shows an inner autophagosome and multiple ER membranes surrounding it, suggesting it is an immature AV. Of note, an additional concentrical structure exhibiting a dense core is also exhibited.